Body temperature protein X-ray crystallography at 37°C: A rhenium protein complex seeking a physiological condition structure.

Francois J.F. Jacobs [a], John R. Helliwell [b *], Alice Brink [a *]

[a.] Department of Chemistry, University of the Free State, Nelson Mandela Drive, Bloemfontein, 9301, South Africa

[b.] Department of Chemistry, University of Manchester, Oxford Road, Manchester M13 9PL, United Kingdom.

Correspondence e-mail: john.helliwell@manchester.ac.uk

Electronic Supplementary Information

Methods

Crystallisation conditions are described in Jacobs et al., 2024 [1] and repeated below:

HEWL (15.0 mg, 1.048 µmol, 1 equivalence) was dissolved in water (0.5 ml). *fac*-$[Et_4N]_2[Re(CO)_3(Br)_3]$ (11.8 mg, 0.015 mmol, 14.6 equivalence) was dissolved in water (0.5 ml). To the metal compound solution, imidazole was added (3.0 mg, 0.0441 mmol, 42.0 equivalence) and dissolved. A buffer solution of 50:50 1.0 M NaCl and 0.05 M sodium acetate buffer at 4.5 pH was prepared. The protein and metal solutions were combined. The protein-metal mixture was treated to 1ml of the buffer solution and gently blended. The protein-metal-buffer solution was transferred to a 96-well sitting drop plate with buffer in the reservoir and the cells sealed. Crystals were collected after 112 weeks for the 37°C dataset, from crystallization setup. In all instances, reproducible crystallization occurred within a week as described in the original publication.[1] Sensitivity of our crystal during data collection at 37°C is noted due to dehydration, X-ray radiation, etc. Practical advice[2] and other suggestions to greasing a crystal to assist the data collection in keeping the crystal stable; and additionally local unfolding of a protein (HEWL) as a function of temp has been studied including up to 325K.[3]

Additional comments: This structural study used co-crystallising protein with the rhenium protocols at room temperature. We did investigate crystallisation at 37°C which is certainly of interest, however the solubility inhibited the finding of crystallisation conditions. That said the high percentage solvent content of the protein crystal allowed the direct visualisation if the bound compounds disassociated from their binding sites; the covalent ones didn't whereas the non-covalent ones did, i.e. with substantially reduced occupancy, and into the solvent channels of the crystal.

HEWL is used as a model protein to explore chemical–structure relationships of rhenium in a biological setting. It is ideal as it provides a nearly complete range of possible amino acids. The caveat being that Cys and Met are not available for coordination as they are either disulfide bonded (Cys) or buried (Met) in HEWL. Although the protein itself is relatively easy to crystallize, the addition of rhenium, an 'unnatural' metal element, in our experience, hinders the crystallization process. SI Fig 1 indicates the three main metal complexations sites which are covalently bound to the protein.

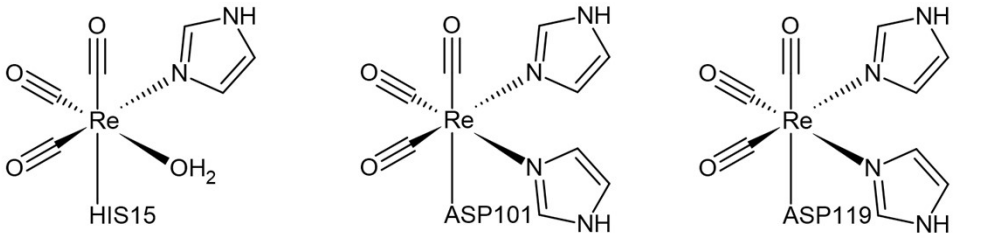

fac-[Re(CO)$_3$(Imi)(H$_2$O)(HIS15)] *fac*-[Re(CO)$_3$(Imi)$_2$(ASP101)] *fac*-[Re(CO)$_3$(Imi)$_2$(ASP119)]

SI Figure 1: Line drawing of the three main metal complexation sites which are covalently bound to the protein.

Crystal sample mounting:

The crystals were carefully removed from the sitting drop by a nylon loop fitted to a magnetic base pin. The crystal was quickly covered by a MiTeGen capillary to prevent dehydration of the crystal. Within the MiTeGen capillary, a few drops of the mother liquor were placed to prevent dehydration, from either the buffer solution, or alternatively deionised water was also found to work well provided no contact was made with the crystal. Prior to crystal mounting the capillary was shortened to prevent collisions within the dual wavelength diffractometer during rotation.

Diffractometer data collection:

The data collection was conducted on a Bruker D8 Venture 4K Kappa Photon III C28 diffractometer fitted with two wavelength sources namely a Mo-Kα X-ray generator with a wavelength of λ = 0.71073 Å and a Cu-Kα anode producing X-ray at λ = 1.54178 Å the latter being used for the data collections of this study. The Oxford temperature control unit allows for high temperature data collections of 37°C.

Data reduction and refinement:

Diffraction data processing was achieved using the Bruker PROTEUM4 software suite, space group determination with POINTLESS[4] and the scaling of the data with AIMLESS.[5] The diffraction resolution cut-off of the data was that suggested by POINTLESS and AIMLESS. The resolution was confirmed by checking to ensure sufficient completeness in the high-resolution shells. Molecular replacement in Phaser[6] and the PDB entry 2w1y [7] were used. Refinement of the molecular models was done using Phenix.[8] Viewing and further optimization was conducted in Coot.[9] The diffraction images indicated the presence of two domains within the selected crystal. The structure was refined from the major domain. The mounted crystal moved within the capillary at frame 45 and data was integrated in two sets (frames 1-45 & 46-90) to accommodate for the slippage. Molecular images were created using UCFS Chimera.[10]

Data availability: The final protein model and the processed diffraction data, as well as the PDB Validation report, are attached to this article or found on the wwPDB. The raw diffraction images zip file is available at Zenodo (https://zenodo.org/) doi: 10.5281/zenodo.13331546. For the highest resolution structure of this complex at 100K the reader is referred to 8QCU held at the wwPDB.

Data accessibility:

For readers not used to accessing PDB files, tutorial videos and guidelines are available at *https://pdb101.rcsb.org*. For use of Zenodo for raw diffraction images deposition and access see Kroon-Batenburg.[11] Additional note, the crystallographic community is still addressing the challenge of interoperability for 2D representation of organometallic complexes extracted from macromolecular data. Automatic software pipelines were developed for large organic molecules (containing C, N, O, H, etc atoms) with well understood organic geometry, however challenges still occur in fully defining metal bonding. The reader should note that the molecular geometry of the

organometallic may be distorted through the automatic macromolecular pipeline servers and are encouraged to review the original paper for the correct metal-based geometry.

Additional comments – metal mechanistic stability at 37°C versus 40°C:

In a clinical setting, the acceptable average for healthy individuals is 37°C, while for an acutely sick patient the patient's temperature may reach 40°C, but such a small change it is unlikely to affect the metal binding of a compound to a protein. From chemical kinetic reaction studies, the substitution rate constant of the organometallic tends to double for each 10°C increase in temperature[12, 13, 14, 15, 16] Chemical mechanistic changes for organometallics, within the temperature range of interest (25-45°C), tend to be solvent, ligand, pH, metal dependent, etc [17, 18, 19, 20, 21] and therefore, to the best of our knowledge, significant rhenium metal binding mechanistic changes are not expected to occur within the limited temperature span of 37 - 40 °C.

Table 1: 1 X-ray crystallographic data and model-refinement statistics for the 37°C crystal structure in comparison to 100K. Statistics for the highest-resolution shell are shown in parentheses.

	100K	37°C
Data reduction		
Space group	$P4_32_12$	$P4_32_12$
Unit cell parameters (Å, °)	81.12(1) 81.12(1) 37.19(3)	81.49(1) 81.49(1) 37.41(3)
	$\alpha = \beta = \gamma = 90$	$\alpha = \beta = \gamma = 90$
Molecules per asymmetric unit	1	1
Detector	Eiger2 XE 16M	Photon III C28
Crystal to detector distance (mm)	168.3	70.0
X-ray source	DLS	Lab Cu Kα
X-ray wavelength (Å)	0.976	1.54
Observed reflections	87971 (7685)	13693 (1276)
Unique reflections	44171 (3979)	6862 (647)
Resolution (Å)	36.28 - 1.15 (1.191 - 1.15)	36.44 - 2.19 (2.27 - 2.19)
Completeness (%)	98.87 (89.54)	99.3 (95.5)
R_{merge}	0.090 (2.098)	0.218 (1.285)
$R_{p.i.m.}$	0.018 (0.854)	0.134 (0.993)
$\langle I/\sigma(I) \rangle$	21.34 (0.78)	5.2 (0.8)
Multiplicity	21.0 (6.4)	6.1 (4.4)
Mn(I) half-set correlation $CC_{1/2}$	0.994 (0.448)	0.985 (0.434)
Cruickshank DPI (Å)	0.022	0.161
Average B-factor (Å²)	23	36
Refinement		
***R* factor**	0.158 (0.3570)	0.2040 (0.3160)
R_{free}	0.177 (0.3969)	0.2712 (0.4024)
R.m.s.d. angles (°)	1.15	1.48
Ramachandran plot values (%)		
Most favoured	98.43	96.06
Additional allowed	1.57	3.94
Disallowed	0.00	0.00
PDB code / Data access	8QCU	9GHX

Table 2. Comparison of all bound ligands (Cl, Na, Re, etc) and waters at 100K and at 37°C specifying B-factors and occupancies where appropriate.

Relevant Residue	**8QCU (100K)**	**B (Å²) 100 K**	**Occup. (%)**		**37 °C**	**B (Å²) C**	**Occup. (%)**	**Notes**
	Cl 201	25	1		Cl 202	50	1	
	Cl 202	23	1		Cl 203	43	1	
	Cl 203	40	1					
	Cl 204	41	1		Cl 211	71	1	
	Cl 216	41	1					
	Br 217	25	1		HOH 31	49	1	Atom in 37°C is offset to 100 K data
	Na 205	22	1		Na 208	36	1	
Covalently Bound Re's								
Asp 101	VHL 206 (Re)	24	0.43		VHL 205 (Re)	78	0.55	
Asp119	VHL 208 (Re)	21	0.53		VHL 204 (Re)	47	0.53	
His 15	REI 207 (Re)	34	0.84		REI 206 (Re)	60	0.94	
Non-covalent Re's								
Asp 18	Re 210	32	0.17		-			No anomalous density
Leu129 /	Re 211	34	0.21		Re 210	47	0.15	

Arg 14								
In vicinity of Arg 14 & His 15	Re 212	21	0.1		Re 209	56	0.15	
	Re 213	21	0.23		Cl 201	34	1	Insufficient anomalous and Fo-Fc density to confirm Re placement.
	Re 214	102	0.26		-			No density to confirm Re placement.
	Re 215	33	0.13		-			No density to confirm Re placement.
Waters								
	HOH 301	25	1					
	HOH 302	37	1					
	HOH 303	30	1					
	HOH 304	36	1					
	HOH 305	28	1					
	HOH 306	34	1					
	HOH 307	30	1					
	HOH 308	38	1					
	HOH 309	38	1					
	HOH 310	26	1					
	HOH 311	22	1		HOH 306	37	1	
	HOH 312	21	1		HOH 304	40	1	
	HOH 313	47	1					
	HOH 314	30	1					
	HOH 315	21	1		HOH 310	40	1	
	HOH 316	31	1					
	HOH 317	28	1		HOH 321	23	1	
	HOH 318	17	1		HOH 309	26	1	
	HOH 319	25	1		HOH 301	54	1	Atom in 37°C is offset from 100 K data
	HOH 320	18	1		HOH 308	28	1	Symmetry equivalent position
	HOH 321	38	1					
	HOH 322	38	1					
	HOH 323	27	1					
	HOH 324	33	1					
	HOH 325	26	1					
	HOH 326	32	1					
	HOH 327	30	1					
	HOH 328	20	1		HOH 302	39	1	
	HOH 329	23	1					
	HOH 330	26	1					
	HOH 331	22	1					
	HOH 332	37	1					
	HOH 333	26	1					
	HOH 334	30	1					
	HOH 335	29	1					
	HOH 336	23	1		HOH 318	36	1	
	HOH 337	27	1					
	HOH 338	30	1					
	HOH 339	28	1					
	HOH 340	31	1					
	HOH 341	30	1					
	HOH 342	46	1					
	HOH 343	28	1					
	HOH 344	29	1					
	HOH 345	44	1					
	HOH 346	23	1					
	HOH 347	36	1					

	HOH 348	24	1					
	HOH 349	20	1		HOH 312	38	1	
	HOH 350	17	1		HOH 311	27	1	
	HOH 351	24	1		HOH 314	40	1	
	HOH 352	27	1					
	HOH 353	39	1					
	HOH 354	28	1					
	HOH 355	40	1					
	HOH 356	41	1					
	HOH 357	29	1					
	HOH 358	24	1		HOH 324	41	1	
	HOH 359	42	1					
	HOH 360	29	1					
	HOH 361	19	1		HOH 325	35	1	Additional HOH in 100 K surrounds this water (333 HOH; 325 HOH). Not observed in 37 °C.
	HOH 362	20	1		HOH 316	21	1	Symmetry equivalent HOH
	HOH 363	38	1		HOH 323	37	1	
	HOH 364	25	1					
	HOH 365	43	1		HOH 326	40	1	
	HOH 366	19	1		HOH 315	25	1	
	HOH 367	34	1		HOH 316	20	1	Atom in 37°C is offset to 100 K data
	HOH 368	33	1		HOH 305	44	1	
	HOH 369	41	1					
	HOH 370	31	1					
	HOH 371	32	1					
	HOH 372	28	1		HOH 320	35	1	
	HOH 373	24	1		HOH 313	36	1	
	HOH 374	23	1					
	HOH 375	32	1					
	HOH 376	35	1					
	HOH 377	38	1					
	HOH 378	35	1		HOH 319	37	1	
	HOH 379	26	1					
	HOH 380	38	1					
	HOH 381	45	1					
	HOH 382	33	1					
	HOH 383	27	1		HOH 322	47	1	100K data interacting with 214 Re.
	HOH 384	25	1					
	HOH 385	37	1					
	HOH 386	25	1					
	HOH 387	35	1					
	HOH 388	40	1					
	HOH 389	29	1					
	HOH 390	38	1					
	HOH 391	42	1					
	HOH 392	44	1					
	HOH 393	25	1					
	HOH 394	38	1					
	HOH 395	35	1					
	HOH 396	35	1					
	HOH 397	36	1					
	HOH 398	46	1					
					HOH 301	52	1	
					HOH 303	40	1	
					HOH 317	42	1	
					HOH 309	49	1	
	Br 217 (sym equivalent)	25	0.23		HOH 327	49	1	
	IMD 209	50-70	1		IMD 207	62-68	1	Imidazole

Table 3: Rhenium occupancy values, anomalous difference map peak heights and residual *Fo*-*Fc* densities as found at 100K and 37°C. The number of weeks soaked in mother liquor as specified by Jacobs et al., 2024 is indicated. At the synchrotron the 38 weeks data were also measured at attenuated intensity and a wavelength identical to CuKα, useful to assess the impact of diffraction resolution in the modelling; see second column at 100K.

Temperature, wavelength and time (in weeks from crystallisation)	100K Week 38 (0.976 Å) 8QCU			100 K Week 38 (1.54 Å)			37°C Week 112, (1.54 Å) 9GHX		
Resolution	1.15 Å			1.76 Å			2.2 Å		
Residue	Σ	P	Δ	Σ	ρ	Δ	Σ	P	Δ
Covalent sites									
HIS15	0.84	55.5	5.5	0.84	35.2	12.1	0.94	6.8	5.4
ASP18	0.17	8.6	-	0.18	5.8	-	-	-	-
ASN46	-	-	-	-	-	-	-	-	-
ASP52	-	-	-	-	-	-	-	-	-
ASP101	0.43	39.4	9.7	0.56	35.2	8.5	0.55	3.6	4.3
ASP119	0.53	54.6	4.0	0.57	30.9	5.0	0.53	5.5	3.5
Other sites									
ARG14/His15	0.10	21.5	6.7	0.17	12.5	4.1	0.15	-	5.1
TYR23	0.23	3.3	3.6	0.31	6.5	-	-	-	-
PRO70	0.13	7.8	-	0.14	5.5	-	-	-	-
ASP101	-	-	-	-	-	-	-	-	-
TRP123	0.26	4.2	-	0.28	3.5	-	-	-	-
ASP129	0.21	9.1	-	0.34	6.1	3.7	0.15	-	4.6

$^{\Sigma)}$ Metal site occupancy; $^{\rho)}$ Anomalous density (σ); $^{\Delta)}$ Residual F_o - F_c density (σ).

References

[1] Jacobs, F. J. F., Helliwell, J. R. & Brink, A. (2024). IUCrJ., 11, 359–373.

[2] Fischer, M. (2021). Q. Rev. Biophys. 54, e1, 1–15.

[3] De Sá Ribeiro, F., Lima., L.M.T.R., (2023). Biophys. Chem., 107027-107039.

[4] Evans, P. R. (2011). Acta. Cryst. D. 67, 282–292.

[5] Evans, P. R., Murshudov, G. N. (2013). Acta. Cryst. D. 69, 1204–1214.

[6] McCoy, A. J. (2007). Acta. Cryst. D. 63, 32–41.

[7] Cianci, M., Helliwell, J. R. & Suzuki, A. (2008). Acta Cryst. D64, 1196–1209.

[8] Liebschner, D., Afonine, P. V., Baker, M. L., Bunkoczi, G., Chen, V. B., Croll, T. I., Hintze, B., Hung, L. W., Jain, S., McCoy, A. J., Moriarty, N. W., Oeffner, R. D., Poon, B. K., Prisant, M. G., Read, R. J., Richardson, J. S., Richardson, D. C., Sammito, M. D., Sobolev, O. V., Stockwell, D. H., Terwilliger, T. C., Urzhumtsev, A. G., Videau, L. L., Williams, C. J. & Adams, P. D. (2019). Acta. Cryst. D. 75, 861–877.

[9] Emsley, P., Lohkamp, B., Scott, W. G. & Cowtan, K. (2010). Acta. Cryst. D. 66, 486–501.

[10] UCFS Chimera (version 1.16), Pettersen, E. F., Goddard, T. D., Huang, C. C., Couch, G. S., Greenblatt, D. M., Meng, E. C. & Ferrin, T. E. (2004). J. Comput. Chem. 25, 1605–1612.

[11] Kroon-Batenburg, L.M.J. (2023), Acta Cryst. F., 79, 267-273.

[12] Brink, A., Visser, H.G., Roodt, A. (2013) Inorg. Chem., 52, 8950- 8961.

[13] Brink, A., Visser, H.G., Roodt, A. (2024) Inorg. Chem., 53, 12480-12488.

[14] Jacobs, FJF., Venter, GJS., Muller, E., Kroon, R.E., Brink, A. (2021) RSC Advance, 11, 24443-24455.

[15] Schutte-Smith, M., Roodt, A., Visser, H.G., (2019) Dalton Trans., 48, 9984-9997.

[16] Schutte-Smith, M., Marker, S.C., Wilson, J.J., Visser, H.G., (2020) Inorg. Chem. 59, 15888−15897.

[17] Roodt, A., Visser, H.G., Brink, A. (2011), Crystallography Reviews, 17, 241-280.

[18] Wilkins, R.G., (1991) Kinetics and Mechanism of Reactions of Transition Metal Complexes, Wiley-VCH Verlag GmbH & Co.

[19] Salignac, B., Grundler, P. V., Cayemittes, S., Frey, U., Scopelliti, R., Merbach, A. E., Hedinger, R., Hegetschweiler, K., Alberto, R., Prinz, U., Raabe, G., Kolle, U., Hall, S. (2003) Inorg. Chem. 42, 3516−3526.

[20] Grundler, P. V., Helm, L., Alberto, R., Merbach, A. E. (2006) Inorg. Chem. 45, 10378−10390.

[21] Pike, S.D., Weller, A.S., (2015), Phil. Trans. R. Soc. A 373, 20140187, 1-24.